79-150

Note: **This is a draft of a paper being submitted for publication. Contents of this paper should not be quoted nor referred to without permission of the authors.**

BAND THEORETIC INTERPRETATION OF NEUTRON SCATTERING EXPERIMENTS IN METALLIC FERROMAGNETS

J. F. Cooke

SOLID STATE DIVISION
OAK RIDGE NATIONAL LABORATORY
Operated by
UNION CARBIDE CORPORATION
for the
U. S. Department of Energy
Oak Ridge, Tennessee

July 1979

[illegible] Interpretation of Neutron Scattering Data from Metallic Ferromagnets*

J.F. [illegible]

[illegible] Ridge National Laboratory, Oak Ridge, Tennessee [illegible], U.S.A.

Magnetic excitations in the 3-d transition metal ferromagnets nickel and iron have been found to possess unusual properties not found in other magnetic systems. For example, inelastic neutron scattering experiments have revealed that spin-waves do not exist at wave-vectors above a particular cut-off value while below this cut-off point they have been observed well above the Curie temperature. This behaviour is not consistent with predictions of localized spin models but can be explained by the band theoretic, or itinerant electron theory. In fact, first principles calculations of the low temperature neutron scattering cross-section based on the itinerant model have been shown to be in excellent agreement with experiment. In addition, the prediction of an optical spin-wave mode has been recently confirmed. The finite temperature extrapolation of the low temperature theory based on the traditional concept of a temperature-dependent spin-splitting of the electronic energy bands appears to be inconsistent with experiment. A more realistic first principles approach to develop a correct finite temperature theory is under investigation.

Neutron scattering experiments have recently revealed some interesting and unusual properties of the spin dynamics of the transition metal ferromagnets nickel and iron, which had not been observed previously in any other magnetic materials. For example, spin-waves were found to exist only in a relatively restricted volume of the Brillouin zone around the zone center, no matter how low the temperature /1, 2/. This disappearance of the spin-wave made as one moves out into the Brillouin zone is inconsistent with theoretical predictions based on the Heisenberg model where spin-waves are found to exist at all wave-vectors for temperatures below the Curie temperature /3/. On the other hand these neutron scattering results are consistent with qualitative predictions based on the itinerant, or band model of magnetism /4/. In fact, these qualitative predictions of the disppearance of spin-waves were partial motivation for the subsequent neutron measurements.

Perhaps even more surprising than the disappearance of spin-waves was the experimental observation that spin-waves existed well above the Curie temperature and that the energy where the spin-waves disappeared, the spin-wave cut-off energy, was independent of temperature /1, 2/. This latter effect indicates that the simple extrapolation of the low temperature itinerant theory to finite temperatures based on the concept of a strong temperature dependent spin-splitting of the electronic energy bands can not be correct.

As we will see the low temperature itinierant theory does seem to provide a good overall qualitative description of the neutron scattering results. However, since the details of how the spin-wave disappears (or indeed whether it disappears at all) is determined by the electronic band structure, it is important that we carry out realistic numerical calculations of the neutron scattering intensity. Such quantitative results can not only help establish the validity of the itinerant theory but also provide an indirect test of the electronic band structure.

Calculations of this type are very difficult to carry out because of the need not only to generate the electronic energies and wave-functions but also to carry out reasonably accurate Brillouin zone sums involving these quantities. Over the years several accurate and efficient methods for generating the electronic band structure have been developed and applied to many materials. Because of problems assosciated with exchange and correlation effects the band structures generated by these numerical procedures are not exact but they can provide "reasonably" good results which can be used as a"realistic" starting point for calculations of the neutron scattering cross-section. The Brillouin zone sums referred to above can also be accurately determined by using analytic computer techniques, such as the Gilat-Raubenheimer /5/ or the tetrahedron methods /6/. Therefore, eventhough the calculation of the neutron scattering intensity involves large scale computer calculation, reasonably accurate numercial results can be obtained in practice.

The purpose of the paper is to briefly outline the itinierant electron theory of magnetism and to present a comparison of some numerical results for the neutron scattering cross-section for ferromagnetic nickel and iron with experiment. The paper is divided into three sections. The general theory is outlined in the first section, numerical results and comparison with experiment are given in the second section, and a summary of conclusions is presented in the last section.

General Theory

The itinerant model of magnetism is based on the concept that the electrons which are responsible for the magnetic properties of a system can be described by an appropriate energy band theory. This is built into the theory from the very beginning by writing the general many electron Hamiltonian in terms of Bloch wave functions $\{\psi_{n\underset{\sim}{k}\sigma}(\underset{\sim}{r})\}$, where n is the band index, $\underset{\sim}{k}$ is a wave-vector, and σ is the spin.

$$\mathcal{H} = \sum_{\substack{m n \\ \underset{\sim}{k}\sigma}} \left(n\underset{\sim}{k}\sigma \left| -\frac{\hbar^2\nabla^2}{2m_e} + U(\underset{\sim}{r}) \right| m\underset{\sim}{k}\sigma\right) C^{\dagger}_{n\underset{\sim}{k}\sigma} C_{m\underset{\sim}{k}\sigma}$$

$$+ \frac{1}{2} \sum_{\substack{n_1 n_2 n_3 n_4 \\ \underset{\sim}{k}_1 \underset{\sim}{k}_2 \underset{\sim}{k}_3 \\ \sigma\sigma'}} \left(n_1 \underset{\sim}{k}_1 \sigma,\ n_2 \underset{\sim}{k}_2 \sigma' \left| \frac{e^2}{|\underset{\sim}{r} - \underset{\sim}{r}'|} \right| n_3 \underset{\sim}{k}_3 \sigma',\ n_4\, \underset{\sim}{k}_1 + \underset{\sim}{k}_2 - \underset{\sim}{k}_3 \sigma\right)$$

$$\times C^{\dagger}_{n_1 \underset{\sim}{k}_1 \sigma} C^{\dagger}_{n_2 \underset{\sim}{k}_2 \sigma'} C_{n_3 \underset{\sim}{k}_3 \sigma'} C_{n_4\, \underset{\sim}{k}_1 + \underset{\sim}{k}_2 - \underset{\sim}{k}_3 \sigma} \qquad (1)$$

$$\langle n\underset{\sim}{k}\sigma | -\frac{\hbar^2\nabla^2}{2m_e} + U(\underset{\sim}{r}) | m\underset{\sim}{k}\sigma\rangle = \int \bar{\psi}_{n\underset{\sim}{k}\sigma}(\underset{\sim}{r})\left[-\frac{\hbar^2\nabla^2}{2m_e} + U(\underset{\sim}{r})\right]\psi_{m\underset{\sim}{k}\sigma}(\underset{\sim}{r})\, d\underset{\sim}{r} \qquad (2)$$

$$\langle n_1\underset{\sim}{k}_1\sigma,\ n_2\underset{\sim}{k}_2\sigma' | \frac{e^2}{|\underset{\sim}{r}-\underset{\sim}{r}'|} | n_3\underset{\sim}{k}_3\sigma',\ n_4\ \underset{\sim}{k}_1+\underset{\sim}{k}_2-\underset{\sim}{k}_3\ \sigma\rangle = \qquad (3)$$

$$\int \bar{\psi}_{n_1\underset{\sim}{k}_1\sigma}(\underset{\sim}{r})\,\bar{\psi}_{n_2\underset{\sim}{k}_2\sigma'}(\underset{\sim}{r}')\frac{e^2}{|\underset{\sim}{r}-\underset{\sim}{r}'|}\,\psi_{n_3\underset{\sim}{k}_3\sigma'}(\underset{\sim}{r}')\,\psi_{n_4\underset{\sim}{k}_1+\underset{\sim}{k}_2-\underset{\sim}{k}_3\sigma}(\underset{\sim}{r})\, d\underset{\sim}{r}\, d\underset{\sim}{r}'$$

The $U(\underset{\sim}{r})$ is the electronic-nuclear potential, m_e is the electron mass, and $C^{\dagger}_{n\underset{\sim}{k}\sigma}(C_{n\underset{\sim}{k}\sigma})$ create (destroy) electrons in the Bloch states $\psi_{n\underset{\sim}{k}\sigma}(\underset{\sim}{r})$.

The quantity we ultimately want to calculate is the inelastic neutron scattering intensity which can be written in terms of the time and space Fourier transform of the dynamic suceptibility /7/, $\chi(\underset{\sim}{q},\omega)$, defined by

$$\chi_{\alpha\beta}(\underset{\sim}{q},\omega) = \frac{1}{2\pi}\int_{-\infty}^{\infty} \langle S^{\alpha}_{\underset{\sim}{q}}(t)\, S^{\beta}_{-\underset{\sim}{q}}(0)\rangle e^{i\omega t}\, dt \qquad (4)$$

where S^{α} is the α component of the total spin operator $\underset{\sim}{S}$, and $\langle\ \rangle$ represents a canonical ensemble average.

The Green's function formalism is used to calculate $\chi_{\alpha\beta}$. We see from Eq. (4) that the Green's function which must be calculated is

$$G_{\alpha\beta}(\underset{\sim}{q},t) = -i\ll T\, S^{-}_{\underset{\sim}{q}}(t)\, S^{+}_{\underset{\sim}{q}}(0)\gg \qquad (5)$$

where T is the time ordering operator. In this paper we are going

to be primarilarly interested in the spin-wave behaviour and, therefore, we need consider only the transverse cross-section for scattering neutrons into the solid angle $d\Omega$ with energy and momentum transfer ω and $\underset{\sim}{q}$ respectively. For low temperatures it can be shown that this cross-section can be directly related to the Green's function $G_{-+}(\underset{\sim}{q},z)$ by the equation

$$\left.\frac{d^2\sigma}{d\Omega\, d\omega}\right|_T \sim Im\left\{\underset{\epsilon\to 0}{Limit}\; G_{-+}(\underset{\sim}{q},\omega+i\epsilon)\right\} \tag{6}$$

where $G_{-+}(\underset{\sim}{q},z)$ is the complex time Fourier transform of

$$G_{-+}(\underset{\sim}{q},t) = -i\langle\langle T\, S^-_{\underset{\sim}{q}}(t)\, S^+_{-\underset{\sim}{q}}(0)\rangle\rangle \tag{7}$$

$$S^{\pm} = S^x \pm i S^y \tag{8}$$

In the Bloch representation we can write

$$G_{-+}(\underset{\sim}{q},t) = \sum_{\substack{n m \\ \underset{\sim}{k}}} \langle n\underset{\sim}{k}\downarrow | e^{-i\underset{\sim}{q}\cdot\underset{\sim}{r}} | m\,\underset{\sim}{k}+\underset{\sim}{q}\uparrow\rangle\, G_2(n\underset{\sim}{k}, m\,\underset{\sim}{k}+\underset{\sim}{q}, t) \tag{9}$$

$$G_2(n\underset{\sim}{k}, m\,\underset{\sim}{k}+\underset{\sim}{q}, t) = -i\langle\langle T\, C^{\dagger}_{n\underset{\sim}{k}\downarrow}\, C_{m\,\underset{\sim}{k}+\underset{\sim}{q}\uparrow}\, S^+_{-\underset{\sim}{q}}(0)\rangle\rangle \tag{10}$$

The calculation of the transverse neutron scattering cross-section is therefore reduced to a calculation of G_2 .

This Green's function is calculated using an equation of motion method. The equation for G_2 is decoupled from the higher order equations by using a generalized RPA decoupling scheme. This approximation neglects spin-wave/spin-wave interactions and certain spin-wave/electron interactions and, therefore, restricts the calculation to low temperatures. At this point we also restrict

the calculation to ferromagnetic materials. The resulting equation for G_2 can be further simplified by requiring that the electronic wave-functions and energies satisfy the following Hartree-Fock-like equations

$$\left\{-\frac{\hbar^2\nabla^2}{2m_e} + U(\underset{\sim}{r}) + \sum_{m\underset{\sim}{\rho}\tau} f_{m\underset{\sim}{\rho}\tau} \int \Psi^{*}_{m\underset{\sim}{\rho}\tau}(\underset{\sim}{r}') \frac{e^2}{|\underset{\sim}{r}-\underset{\sim}{r}'|} \Psi_{m\underset{\sim}{\rho}\tau}(\underset{\sim}{r}')\, d\underset{\sim}{r}'\right\} \Psi_{n\underset{\sim}{k}\sigma}(\underset{\sim}{r})$$

$$- \sum_{m\underset{\sim}{\rho}} f_{m\underset{\sim}{\rho}\sigma}\, \Psi_{m\underset{\sim}{\rho}\sigma}(\underset{\sim}{r}) \int \Psi^{*}_{m\underset{\sim}{\rho}\sigma}(\underset{\sim}{r}')\, U_{sc}(\underset{\sim}{r},\underset{\sim}{r}')\, \Psi_{n\underset{\sim}{k}\sigma}(\underset{\sim}{r}')\, d\underset{\sim}{r}' \qquad (11)$$

$$= E(n\underset{\sim}{k}\sigma)\, \Psi_{n\underset{\sim}{k}\sigma}(\underset{\sim}{r})$$

The quantity f is the Fermi occupation number and $U_{sc}(\underset{\sim}{r},\underset{\sim}{r}')$ is a non-local screened electron-electron interaction. The theory dictates how U_{sc} is to be calculated but the procedure is too difficult to carry out in practice. We assume, therefore, that Eq. (11) is sufficently general so that a realistic energy band structure can be obtained for some appropriate choice of U_{sc}. The specific procedure we use to deal with the problem will be described later on in this section.

With $\Psi_{n\underset{\sim}{k}\sigma}(r)$ and $E(n\underset{\sim}{k}\sigma)$ determined from Eq. (11) the equation for the complex time transform of G_2 reduces to

$$\left\{z - E(n\underset{\sim}{k}\downarrow) + E(m\,\underset{\sim}{k}+\underset{\sim}{q}\uparrow)\right\} G_2(n\underset{\sim}{k}, m\,\underset{\sim}{k}+\underset{\sim}{q}, z)$$

$$= \hbar\,(n\underset{\sim}{k}\downarrow|\, e^{-i\underset{\sim}{q}\cdot\underset{\sim}{r}}\,|m\,\underset{\sim}{k}+\underset{\sim}{q}\uparrow)\left\{f_{n\underset{\sim}{k}\downarrow} - f_{m\,\underset{\sim}{k}+\underset{\sim}{q}\uparrow}\right\} \qquad (12)$$

$$-\left\{f_{n\underset{\sim}{k}\downarrow} - f_{m\,\underset{\sim}{k}+\underset{\sim}{q}\uparrow}\right\} \sum_{i\underset{\sim}{\rho}} (m\,\underset{\sim}{k}+\underset{\sim}{q}\uparrow,\, i\underset{\sim}{\rho}\downarrow|\, U_{sc}(\underset{\sim}{r},\underset{\sim}{r}')\,|n\underset{\sim}{k}\downarrow,\, j\,\underset{\sim}{\rho}+\underset{\sim}{q}\uparrow)\, G_2(i\underset{\sim}{\rho}, j\,\underset{\sim}{\rho}+\underset{\sim}{q}, z)$$

In order to solve this equation we must find some reasonable approximation for the screened coulomb matrix element. The simplest approximation to make is to treat it as a constant,

say I_o. With this approximation the Eq. (12) can be solved and the scattering intensity determined. The result for a single band magnet for scattering vector $\underset{\sim}{Q} = \underset{\sim}{q} + \underset{\sim}{\tau}$, $\underset{\sim}{\tau}$ a reciprocal lattice vector and $\underset{\sim}{q}$ restricted to the first Brillouin zone, is

$$\frac{d^2\sigma}{d\Omega d\omega}\Big|_T \sim \frac{\chi_o''(\underset{\sim}{q},\omega)}{\{1 - I_o \chi_o'(\underset{\sim}{q},\omega)\}^2 + \{I\chi_o''(\underset{\sim}{q},\omega)\}^2} \tag{13}$$

$$\chi_o(\underset{\sim}{q},\omega) = \underset{\epsilon \to o}{\text{Limit}} \frac{1}{N} \sum_{\underset{\sim}{k}}' \frac{f_{k\downarrow} - f_{\underset{\sim}{k}+\underset{\sim}{q}\uparrow}}{\omega - E(\underset{\sim}{k}\downarrow) + E(\underset{\sim}{k}+\underset{\sim}{q}\uparrow) + i\epsilon} \tag{14}$$

$$= \chi_o'(\underset{\sim}{q},\omega) - i\chi_o''(\underset{\sim}{q},\omega) \tag{15}$$

A similar approximation in Eq. (11) yields

$$E(\underset{\sim}{k}\sigma) = \varepsilon(\underset{\sim}{k}) + I_o(n_{-\sigma} - n_\sigma) \tag{16}$$

where n_σ is the number of electrons with spin σ

$$n_\sigma = \sum_{\underset{\sim}{k}}' f_{\underset{\sim}{k}\sigma} \tag{17}$$

and $\varepsilon(\underset{\sim}{k})$ would have been the energy of the electrons had the system been non-magnetic $(n_\uparrow = n_\downarrow)$.

The result given in Eq. (13) is the well known enhanced susceptibility result derived originally by Izuyama, Kim and Kubo /4/. In order to understand what spin-waves are and why they disappear we need to examine this expression in some detail.

The behaviour of the scattering cross-section is determined to a great extent by $\chi_o''(\underset{\sim}{q},\omega)$. From Eqs.(14) and (15) we see

that this function is simply related to the total density of states for a spin flip transition of a electron across the Fermi surface with a fixed momentum change $\underset{\sim}{q}$.

$$\chi_o''(\underset{\sim}{q},\omega) = \pi \sum_{\underset{\sim}{k}}' \{ f_{\underset{\sim}{k}\downarrow} - f_{\underset{\sim}{k}+\underset{\sim}{q}\uparrow} \} \delta(\omega - E(\underset{\sim}{k}\downarrow) + E(\underset{\sim}{k}+\underset{\sim}{q}\uparrow)) \tag{18}$$

Such excitations are called Stoner excitations. Notice that for $|\underset{\sim}{q}| \to 0$

$$\chi_o''(0,\omega) = \pi (n_\downarrow - n_\uparrow) \delta(\omega - \Delta) \tag{19}$$

$$\Delta = E(k\downarrow) - E(k\uparrow) = (n_\uparrow - n_\downarrow) I_o = \text{constant} \tag{20}$$

where Δ is called the spin-splitting parameter. Clearly, $\chi_o'' = 0$ unless $\omega = \Delta$. As $\underset{\sim}{q}$ is inecreased χ_o'' will be non-zero only between some maximum and minimum energies. The region of $(\underset{\sim}{q},\omega)$ space where χ_o'' is non-zero is called the Stoner continuum and is sketched in Fig. 1. For $(\underset{\sim}{q},\omega)$ outside the Stoner continuum the scattering intensity is zero except where

$$1 - I_o \chi_o'(\underset{\sim}{q},\omega) = 0 \tag{21}$$

For this case a limiting procedure yields a delta function singularity in the scattering intensity located at the solution of Eq. (21). This is just the spin-wave peak and,therefore, Eq. (21) locates the spin-wave dispersion curve. The spin-wave energy can be shown to be quadratic in $\underset{\sim}{q}$ ar is also sketched in Fig. 1.

The explanation of the disappearance of spin-waves is now quite

simple. Since the condition given in Eq. (21) leads to poles in the two-body Green's function, G_2, it follows that the spin-waves in this theory are bound states between an electron of a given spin and a hole of opposite spin. If the spin-wave dispersion curve enters the Stoner continuum then this bound electron-hole pair is degenerant in energy with single-particle Stoner excitations and the spin-wave will decay. The lifetime (or line width) will depend obviously on the Stoner density of states. These results are consistent which the formula in Eq. (13) because if we are in the Stoner continuum then $\chi_0'' \neq 0$ and the spin-wave line will broaden by an amount which depends on the magnitude of $I_0 \chi_0''$. These results also point out the need for carrying out numerical calculations because the shape and position of the Stoner continuum depends on the details of the band structure. For example, if the Stoner continuum lies very high in energy then the spin-wave will be well defined at all $\underset{\sim}{q}$, while if it lies low in energy the spin-wave may exist for only very small $\underset{\sim}{q}$.

Before turning to the problem of numerically evaluating the scattering cross-section we need to reconsider the matrix element approximation. Unfortunately the constant matrix element approximation can not be very good for transition metal systems because of the relatively strong band and wave-vector dependence of the Bloch functions. Several years ago the author suggested a method of including these effects in a approximate way /8/ by using an interpolation expansion for the wave-function. This method can also be based on the Korringa, Kohn, Rostocker (KKR) wave-function expansion

$$\psi_{n\underset{\sim}{k}\sigma}(\underset{\sim}{r}) = \sum_{\mu} a_{n\mu\sigma}(\underset{\sim}{k})\, \phi_{\mu}(\underset{\sim}{r}) \qquad (22)$$

where μ represents a combined angular momentum index (ℓ, m). The $a_{n\mu\sigma}(\underset{\sim}{k})$ are expansion coefficients and the ϕ_μ are products of radial functions and spherical harmonics. Substitution of this expansion into the screened coulomb matrix element expression allows us to separate the band and wave-vector dependence given by the expansion coefficients from $U_{sc}(\underset{\sim}{r}, \underset{\sim}{r}')$ which occurs in symmetry dependent integrals over the unit cell. Since U_{sc} is not known we treat these unit cell integrals as parameters which are adjusted to yield a reasonable band structure for the system of interest. The number of such symmetry dependent parameters is initially large but it can be reduced considerably by relying on order of magnitude and symmetry arguments. In the work presented here we have ignored the effects of the spin-splitting of the s and p symmetry states and have chosen to describe the splitting of the d-symmetry states with two parameters, V_1 for e_g and V_2 for t_{2g} symmetry.

The general expression for the electronic energy which is generated by these approximations is

$$E(n\underset{\sim}{k}\sigma) = \varepsilon(n\underset{\sim}{k}\sigma) + \sum_{\mu}{}' |a_{n\mu\sigma}(\underset{\sim}{k})|^2 \{ h_\mu^\sigma - h_\mu^P \} \tag{23}$$

$$h_\mu^\sigma = \frac{W_\mu}{N} \sum_{m\underset{\sim}{\ell}}{}' |a_{m\mu\sigma}(\underset{\sim}{\ell})|^2 f_{m\underset{\sim}{\ell}\sigma} \tag{24}$$

The function $\varepsilon(n\underset{\sim}{k}\sigma)$ has a very weak spin-dependence arising from the explicit spin-dependence of the electronic wave functions which can generally be neglected. The major spin-dependence comes from the second term in which the sum on is restricted to only the 5 d-symmetry terms and $W_\mu = V_1 (V_2)$ for $e_g (t_{2g})$ symmetry. The function h_μ^P is h_μ^σ evaluated in the paramag-

netic band structure. If we put $V_1 = V_2$ the result in Eq. (23) reduces to the form for $E(n\underset{\sim}{k}\sigma)$ proposed by Hodges, Ehrenreich and Lang, based on their interpolation scheme.

The matrix element approximations which have been made also local to a closed form expression for the Green's function $G_{-+}(\underset{\sim}{q}, z)$. The result is

$$G_{-+}(\underset{\sim}{q}, z) = \sum_{\mu\nu\underset{\sim}{l}}{}' F_\mu(\underset{\sim}{q}) \left[I + \Gamma(\underset{\sim}{q}, z) W \right]^{-1}_{\mu\nu} \Gamma_{\nu\eta}(\underset{\sim}{q}, z) \bar{F}_\eta(\underset{\sim}{q}) \tag{25}$$

$$F_\mu(\underset{\sim}{q}) = \int |\phi_\mu(\underset{\sim}{r})|^2 e^{-i\underset{\sim}{q}\cdot\underset{\sim}{r}} \, d\underset{\sim}{r} \tag{26}$$

$$(\Gamma W)_{\mu\nu} = \frac{W_\nu}{N} \sum_{\substack{nm \\ \underset{\sim}{k}}}{}' \frac{a_{n\mu\downarrow}(\underset{\sim}{k}) \, a_{m\mu\uparrow}(\underset{\sim}{k}+\underset{\sim}{q}) \, a_{n\nu\downarrow}(\underset{\sim}{k}) \, a_{m\nu\uparrow}(\underset{\sim}{k}+\underset{\sim}{q}) \left\{ f_{n\underset{\sim}{k}\downarrow} - f_{m\,\underset{\sim}{k}+\underset{\sim}{q}\uparrow} \right\}}{z - E(n\underset{\sim}{k}\downarrow) + E(m\underset{\sim}{k}+\underset{\sim}{q}\uparrow)} \tag{27}$$

These results are considerably more complicated than the constant matrix element results discussed earlier. It should be noted here that no new parameters hve been introduced beyond those already incorporated in the band calculation. Therefore, once the band structure is given the dynamics of the spin system is uniquely determined. The method of determining theses parameters will be discussed in the next section.

Numerical Results

The first step in carrying out a numerical calculation of the neutron scattering intensity is to determine the ferromagnetic band structure. At least two different methods can be used within the framework of this theory. Both methods begin with a "realistic" conventional non-magnetic, or paramagnetic, energy band calculation. One approach is then to fit these bands with a Hodges-Ehrenreich, Lang or Slater-Koster interpolation scheme. Then we can write

$$\sum_{\nu} H_{\mu\nu}(\underset{\sim}{k})\, a_{n\nu}(\underset{\sim}{k}) = \varepsilon(n\underset{\sim}{k})\, a_{n\mu}(\underset{\sim}{k}) \qquad (28)$$

where $H_{\mu\nu}$ is the interpolation matrix that describes the non-magnetic states, and $\varepsilon(n\underset{\sim}{k})$ and $a_{n\mu}(\underset{\sim}{k})$ are the corresponding energies and wave-function expansion coefficients.

The ferromagnetic bands can then be generated from the equation

$$\sum_{\nu} \{ H_{\mu\nu}(\underset{\sim}{k}) + \delta_{\mu,\nu}[h_{\mu}^{\sigma} - h_{\mu}^{\rho}] \}\, a_{n\nu\sigma}(\underset{\sim}{k}) = \varepsilon(n\underset{\sim}{k}\sigma)\, a_{n\mu\sigma}(\underset{\sim}{k}) \qquad (29)$$

If this equation is multiplied through by $a_{n\mu\sigma}(\underset{\sim}{k})$ and summed on μ we recover the general result given in Eq.(23). In order to carry out the band calculation we must first specify the two parameters V_1 and V_2 and then solve Eq. (29) self-consistently, since h_{μ}^{σ} depends on the $a_{n\mu\sigma}(\underset{\sim}{k})$. The total spin only moment

$$\delta n = n_{\uparrow} - n_{\downarrow} = \sum_{n\underset{\sim}{k}} \{ f_{n\underset{\sim}{k}\uparrow} - f_{n\underset{\sim}{k}\downarrow} \} \qquad (30)$$

and the number of electrons of symmetry type μ

$$n_\mu^\sigma = \sum_{n\underset{\sim}{k}} |a_{n\mu\sigma}(\underset{\sim}{k})|^2 f_{n\underset{\sim}{k}\sigma} \qquad (31)$$

can be calculated. We then choose V_1 and V_2 so that we get the experimentally determined values of δn and n_μ^σ /9/.

Detail numerical calculations based on this model have shown that, to a good approximation, the spin-dependence of the expansion coefficients can be ignored. This result suggest an alternate approach for carrying out the calculation without having to rely on the interpolation schemes. This method is to replace $a_{n\mu\sigma}(\underset{\sim}{k})$ and $\varepsilon(n\underset{\sim}{k}\sigma)$ in Eq. (23) by their paramagnetic counterparts, $a_{n\mu}(\underset{\sim}{k})$ and $\varepsilon(n\underset{\sim}{k})$, and then to iterate Eq. (23) to convergence for fixed values of V_1 and V_2. The values for V_1 and V_2 are to be determined as described previously. Both mehtods have been found to give essentially the same ferromagnetic band structure.

Examples of the type of band structures which can be obtained from these procedures are given in Figs. (2) and (3) for nickel and iron respectively. Both calculations yield a complex of d bands which hybridize with a broad s-like band. The calculation for nickel was based on paramagnetic bands proposed by Stocks, Faulkner, and Williams /10/. The dotted lines refer to minority spin bands while the solid lines are majority spin bands.

Because of the approximations which have been made the energy bands along a given direction are rigidly spin split if the electronic wave-function expansion along that direction contains only symmetry terms which belong to the same irreducible representation. For example, along Γ to X we find bands with pure e_g symmetry which are spin-split by about .1 eV and bands with pure t_{2g} symmetry which are split by about .4 eV. This rather different splitting of these two sets of bands gives rise to only one hole pocket at X , in agreement with experiment. Most band calculations for nickel yield comparable splitting for these particular bands and, therefore, two pockets at X . For bands where the wave-function expansion contains symmetry terms from more than one irreducible representation rather strong wave-vector-dependent splitting can occur as one varies $\underset{\sim}{k}$.

The calculation for iron was based on paramagnetic bands proposed by Wood /11/. Again the dotted lines refer to minority spin bands. In contrast to the nickel results the e_g and t_{2g} spin-splittings were found to be approximately the same, which results in an almost rigid splitting ($\sim$ 2 eV) of the d-symmtry bands. The wave-vector-dependent splitting obtained in the iron bands results almost entirely from hybridization effects.

Given these energy bands the Green's function $G_{-+}(\underset{\sim}{q},z)$, given in Eq. (25), and thus the neutron scattering cross-section can now be evaluated numerically. Extensive calculations have been carried out along the three principle symmetry directions for both nickel and iron. Because of the complexity of these calculations no attempt was made to adjust V_1 and V_2 to obtain a "best fit" to the data. Such calcu-

lations could, in principle, be undertaken but would require unrealistic amounts of computer time.

Results for the transverse neutron scattering cross-section for nickel are shown in Fig. (4). These results were obtained for $\underset{\sim}{q}$ along [100] and show two interesting features. The spin-wave peak which is sharp at low $\underset{\sim}{q}$ broadens and becomes smaller for large $\underset{\sim}{q}$. Also at the larger values of $\underset{\sim}{q}$ two distinct peaks can be observed. The spin-wave dispersion curve obtained from the peak positions is shown in Fig. (5). There are two branches, one acoustic and one "optic", which appear to interact. The absence of any scattering intensity in the "optic" mode at low $\underset{\sim}{q}$ follows from an exact sum rule that all of the scattering must be in the acoustic mode at $\underset{\sim}{q} = 0$ /8/. The acoustic branch bends over and, as can be seen from Fig. (4), a small peak persists out to the zone boundary. The low $\underset{\sim}{q}$ part of the dispersion curve is seen to be in excellent agreement with experiment /1/. The "optic" branch and the persistence of the acoustic branch out to the zone boundary were not observed in the original experiments possibly because of the relative poor counting statistics at these high energies ($\sim$120 meV). In a recent exeperiment Mook has improved the statistics by using a larger crystal and the hot source on the high flux reactor at the ILL and has observed the "optic" mode dispersion curve as predicted by the theory /12/. The bending over of the acoustic branch was also observed but not the persistence of the mode out to the zone boundary. In order to determine if this peak could be observed in a neutron experiment we must fold in the experimental resolution function. Unfortunately this can not be done at present because of the amount of computer time

this would require. The scattering intensity along [110] and [111] was found to drop to zero in a manner identical to that found for iron, which is described below. The spin-wave dispersion curve was found to be isotropic in $\underset{\sim}{q}$ and the spin-waves were found to disappear at about 100 meV in excellent agreement with experiment.

The neutron scattering cross-section calculated for iron is plotted in Fig. (6) for $\underset{\sim}{q}$ along [100]. The results for $\underset{\sim}{q}$ along [110] and [111] were found to be essentially the same as along [100] . In contrast to the [100] nickel results the spin-wave peak continues to drop until it completely disappears. The dispersion curve obtained from the peak positions is shown in Fig. (7). Again the agreement between theory and experiment is seen to be excellent. In addition, the predicted disappearance of the spin-wave peak is in good agreement with the measurements of Mook et al. /2/.

The calculations described above were carried out at zero temperature. The extension of these results to finite temperatures is very difficult because the theory must be carried beyond RPA. For this reason the finite temperature theory has, in the past, developed along the lines of a simple extrapolation of the low temperature theory. This extrapolation leads to the conclusion that the spin-splitting is temperature dependent and vanishes at the Curie temperature where $n_\uparrow = n_\downarrow$ (see e.g. Eq. (20)) Numerical calculations based on the models carried out by Lowde and Windsor /13/, and later by the author, indicate that the Stoner continuum will move down in energy as the temperature is raised. This in time would require that the spin-wave cut-off

energy would also be temperature dependent, which is not the case found experimentally. It appears, therefore, that this simple temperature extrapolation of the low temperature theory can not be correct. The development of suitable finite temperature theory must not only lead to a temperature independent spin-wave cut-off energy but also the existence of spin-waves well above the Curie temperature. The development of such a theory is currently under investigation.

Conclusions

The itinerant theory of magnetism has been shown to provide an excellent quantitative as well as qualitative model for decribing the low temperature spin dynamics of the transition metal ferromagnets nickel and iron. Calculations of the transverse inealstic neutron scattering cross-section have been found to be in good agreement with experiment both with respect to the spin-wave dispersion curves and the disappearance phenomena. These calculations were based on an generalized RPA decoupling scheme and on the use of an approximate procedure for incorporating the band and wave-vector dependence of relevant matrix elements. Numerical investigations of this later effect indicate that it is important, i.e. the constant matrix element approximation is not appropriate for nickel and iron.

This matrix element approximation has also been found to lead to a strong band and wave-vector dependent splitting of the

electronic energy bands and a rather complicated expression for the scattering intensity, in contrast to the rigid splitting-enhanced susceptibility results generated by the constant matrix element approximation. By introducing the matrix which diagonalizes $[I + \Gamma W]$ in Eq. (25) it is straightforward to show that it is a weighted Stoner density of states which controls the disappearance of the spin-waves and not the total Stoner density of states. The simple picture of the spin-wave running into the "Stoner continuum" is therfore correct only if we view the "Stoner continuum" as a region in $(\underset{\sim}{q}, \omega)$ space where a suitably weighted Stoner density of states is large.

It has also been argued that the extrapolation of the low temperature theory by using a temperature dependent splitting parameter is not consistent with neutron scattering results. The extension of these low temperature calculations to higher temperatures must await the development of a realistic high temperature theory.

Acknowledgement

The author would like to thank the Institute für Festkörperforschung at Kernforschungsanlage Jülich for its hospitality during the preparation of this manuscript.

References

/1/ H.A. Mook, R.M. Nicklow, E.D. Thompson, and M.K. Wilkinson
J. Appl. Phys. 40, 1450 (1969).
H.A. Mook, J.W. Lynn, and R.M. Nicklow
Phys. Rev. Lett. 30, 556 (1975);
AIP Conf. Proc. 18, 781 (1974)
J.W. Lynn and H.A. Mook
(to be published)

/2/ H.A. Mook and R.M. Nicklow,
Phys. Rev. B 1, 336 (1973)
J.W. Lynn,
Phys. Rev. B 11, 2624 (1975)

/3/ See, for example, the review by
C. Herring in Magnetism, ed. by G.T. Rado and H. Suhl
(Academic, N.Y. 1967), Vol. 4

/4/ T. Izuyama, D. Kim, and R. Kubo
J. Phys. Soc. Japan 18, 1025 (1963)

/5/ G. Gilat and L.J. Raubenheimer,
Phys. Rev. 144, 390 (1966)

/6/ G. Lehman and M Taut,
phys. stat. sol. 54, 469 (1972)

/7/ W. Marshall and S.W. Lovesey
Theory of Thermal Neutron Scattering, (University Press, Oxford, 1971)

/8/ J.F. Cooke,
Phys. Rev. B 7 1108 (1973)

/9/ H. Daman, A. Herr, and A.J.P. Meyer,
J. Appl. Phys. 39, 669 (1968)
G. G. Scott
Rev. Mat. Phys. 34, 102 (1962).
H.A. Mook
Phys. Rev. 148, 495 (1966)
C.G. Shull, in
Electronic Structure and Alloy Chemistry of Transition Elements
ed. by P.A. Beck (Interscience, 1963) pg 15
C.G. Shull and H.A. Mook,
Phys. Rev. Lett. 16, 184 (1966)

/10/ G.M. Stocks, R.W. Williams, and J.S. Faulkner,
Phys. Rev. B 4, 4390 (1971)

/11/ J.H. Wood
Phys. Rev. 126, 517 (1962)

/12/ H.A. Mook
to be published

/13/ R.D. Lowde and C.G. Windsor
Adv. in Phys. 19, 813 (1970)

Figure Captions

Figure 1: Schematic drawing of the Stoner continuum and the spin-wave dispersion curve for a single band itinerant ferromagnet

Figure 2: Energy bands for ferromagnetic nickel

Figure 3: Energy bands for ferromagnetic iron

Figure 4: Transverse inelastic neutron scattering intensity for ferromagnetic nickel plotted as a function of energy for fixed values of $\underset{\sim}{q}$ (in units of $2\pi/a_o$) along [100] .

Figure 5: Spin-wave dispersion curve for ferromagnetic nickel for $\underset{\sim}{q}$ (in units of $2\pi/a_o$) along [100] . The experimental points ⟷ are those of H.A. Mook et al., Phys. Rev. Lett. 30, 556 (1973)

Figure 6: Transverse inelastic neutron scattering intensity for ferromagnetic iron plotted as a function of energy for fixed values of $\underset{\sim}{q}$ (in units of $2\pi/a_o$)

Fig. 7: Spin-wave dispersion curve for ferromagnetic iron for $\underset{\sim}{q}$ (in units of $2\pi/a_o$) along [100] .

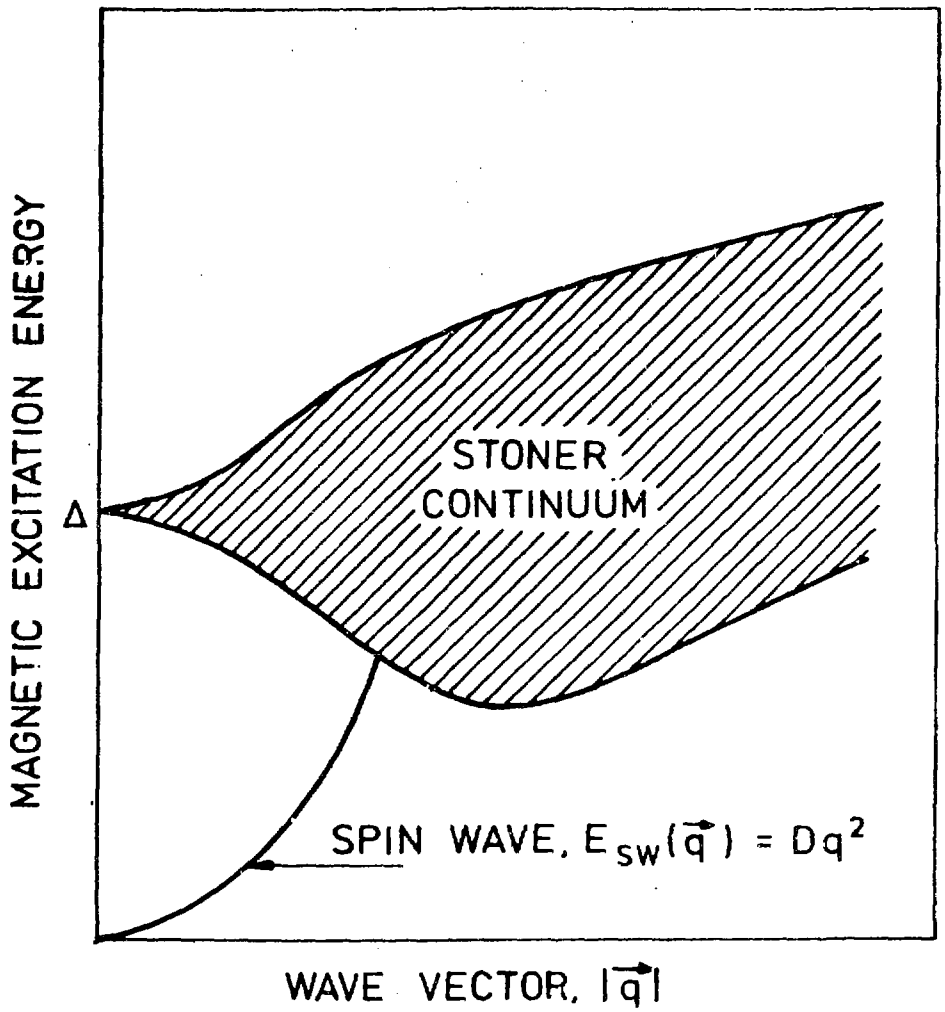
MAGNETIC EXCITATION ENERGY
Δ
STONER
CONTINUUM
SPIN WAVE, $E_{SW}(\vec{q}) = Dq^2$
WAVE VECTOR, $|\vec{q}|$

Fig 1

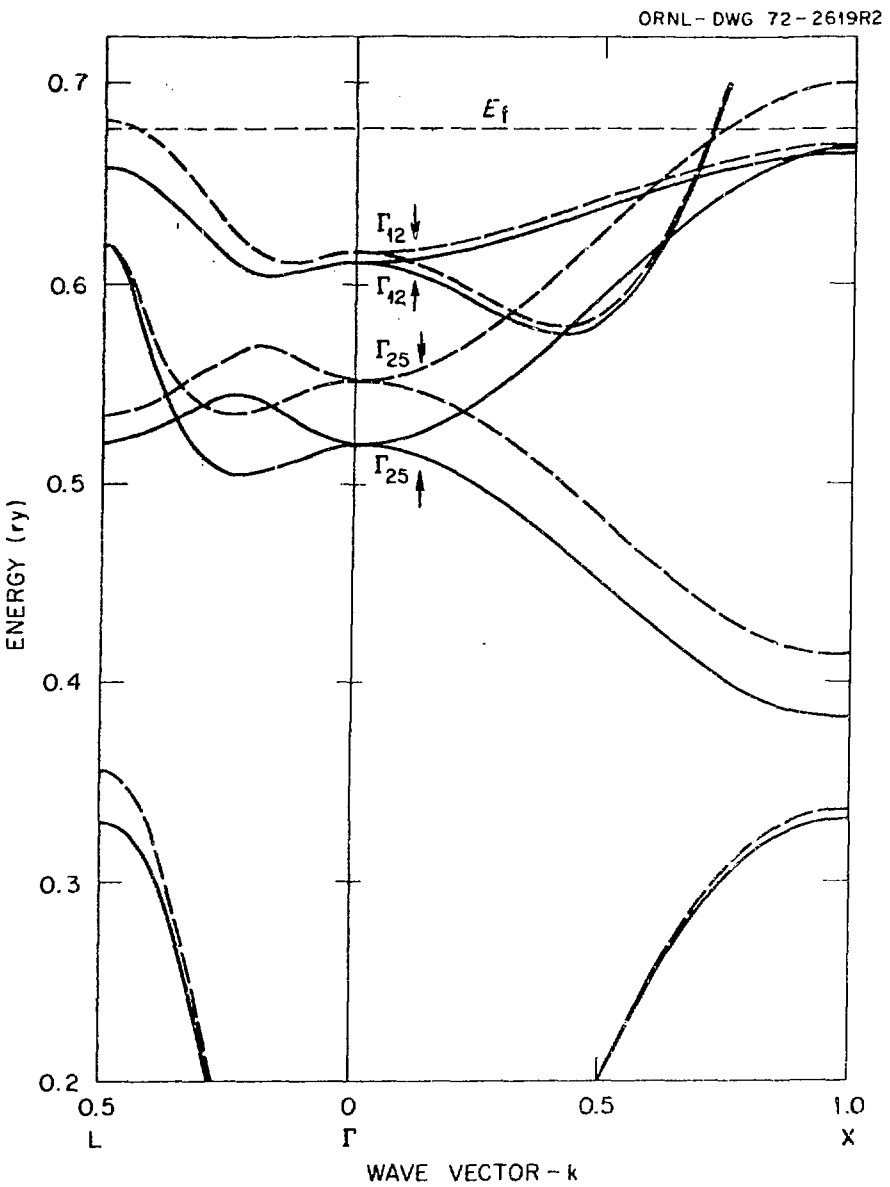
ORNL - DWG 72 - 2619R2
0.7
0.6
0.5
0.4
0.3
0.2
E_f
$\Gamma_{12}\downarrow$
$\Gamma_{12}\uparrow$
$\Gamma_{25}\downarrow$
$\Gamma_{25}\uparrow$
ENERGY (ry)
0.5
0
0.5
1.0
L
Γ
X
WAVE VECTOR - k

Fig 2

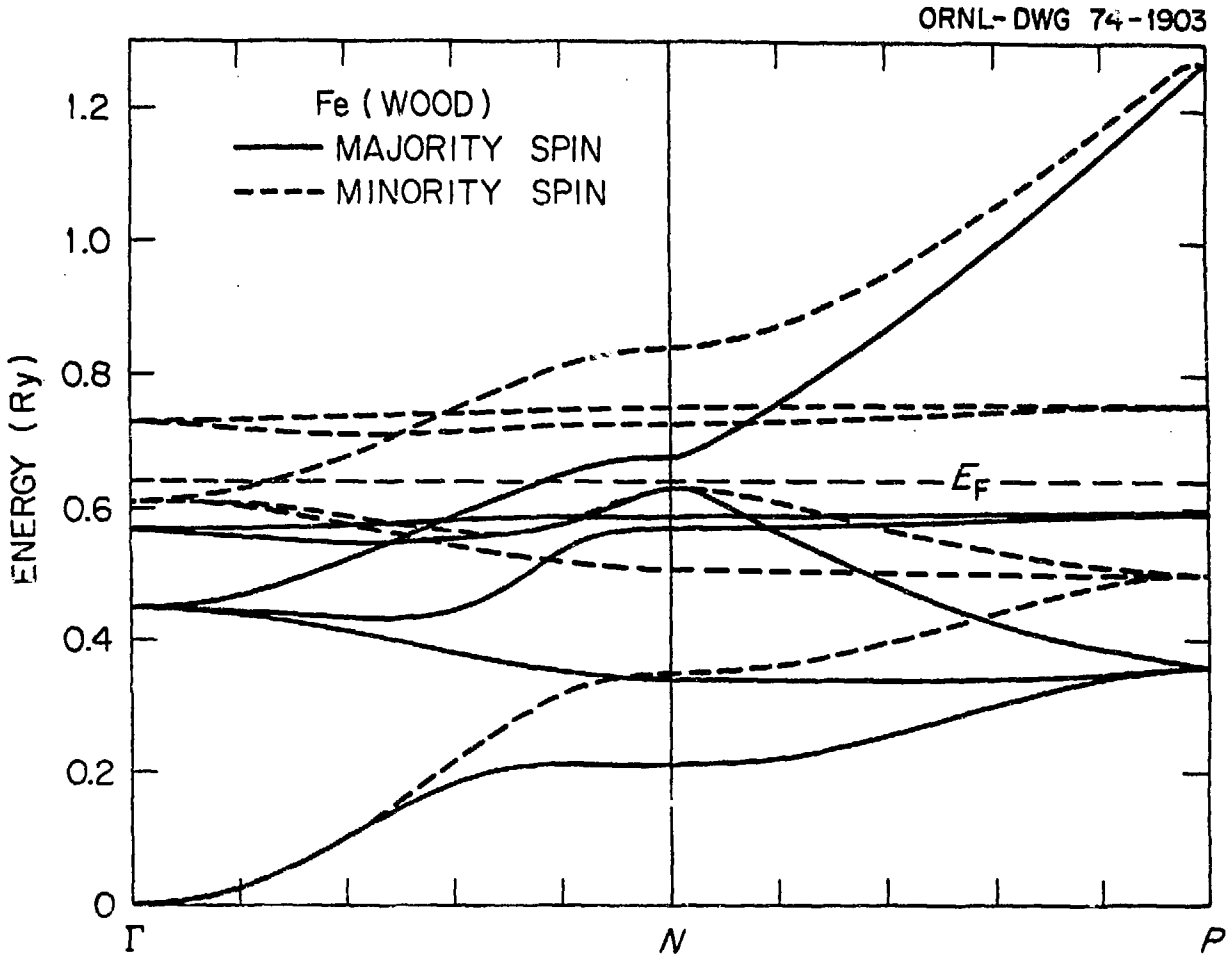
ORNL-DWG 74-1903
Fe (WOOD)
MAJORITY SPIN
MINORITY SPIN
ENERGY (Ry)
1.2
1.0
0.8
0.6
0.4
0.2
0
E_F
Γ
N
P

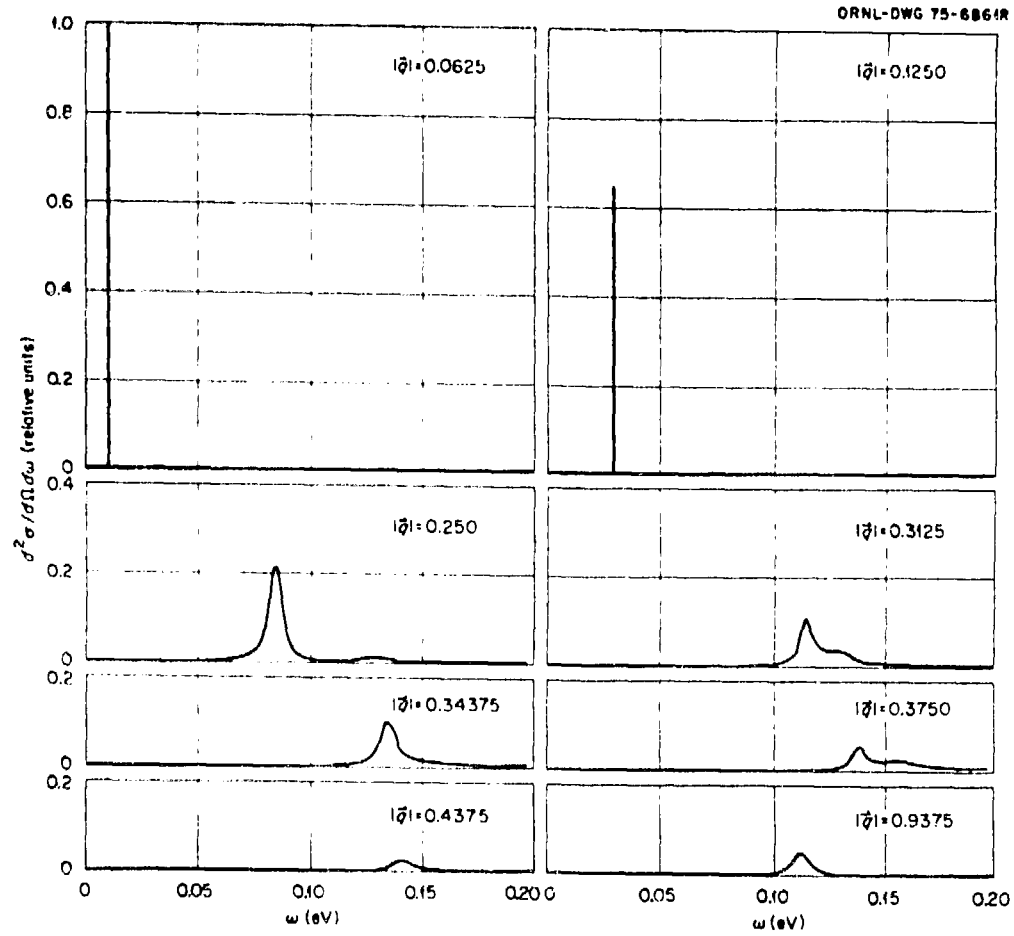
ORNL-DWG 75-6861R
$|\vec{q}|$=0.0625
$|\vec{q}|$=0.1250
$|\vec{q}|$=0.250
$|\vec{q}|$=0.3125
$|\vec{q}|$=0.34375
$|\vec{q}|$=0.3750
$|\vec{q}|$=0.4375
$|\vec{q}|$=0.9375
$d^2\sigma/d\Omega d\omega$ (relative units)
ω (eV)
ω (eV)

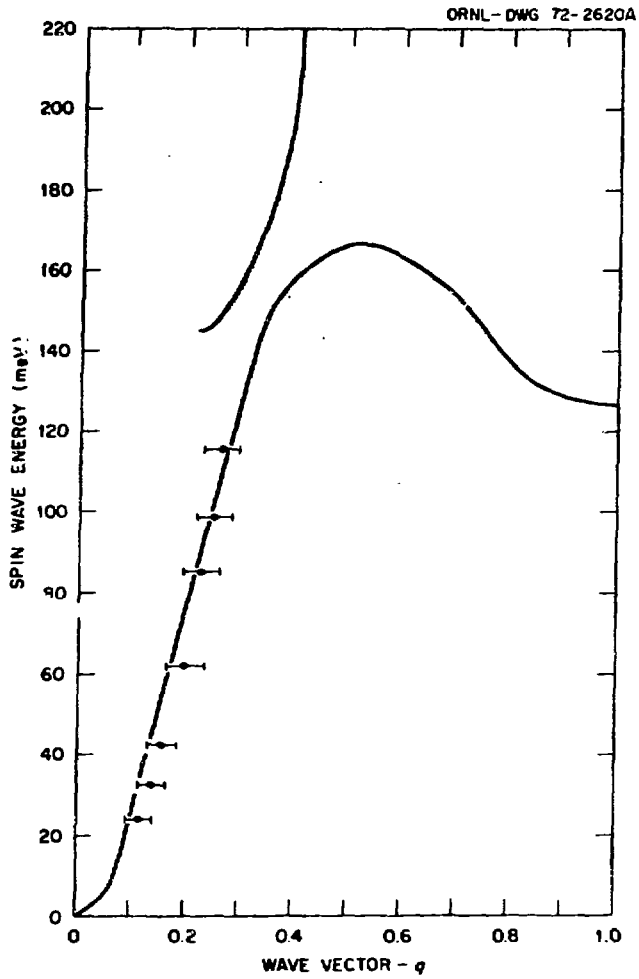

Spin Wave Energy in Nickel – 100.

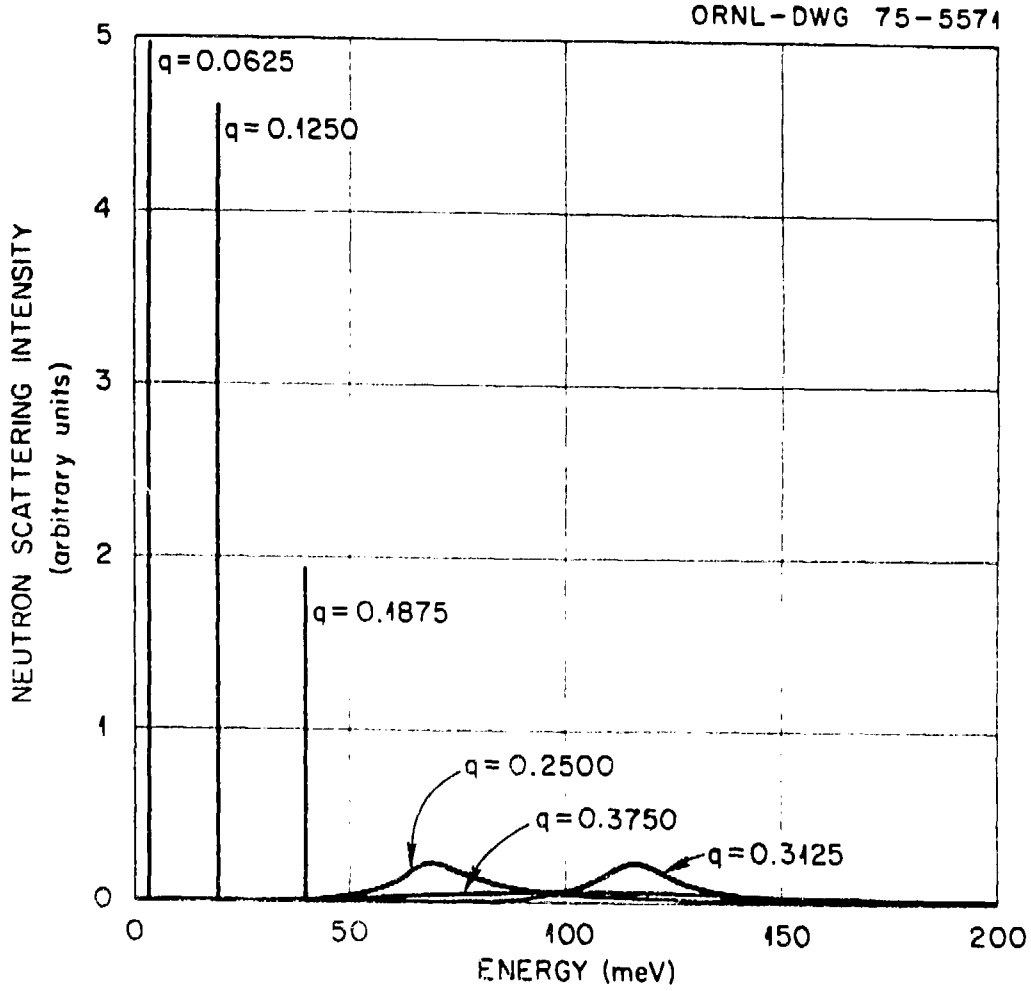
ORNL-DWG 75-5571
NEUTRON SCATTERING INTENSITY
(arbitrary units)
ENERGY (meV)
q = 0.0625
q = 0.1250
q = 0.1875
q = 0.2500
q = 0.3750
q = 0.3125
0
1
2
3
4
5
0
50
100
150
200

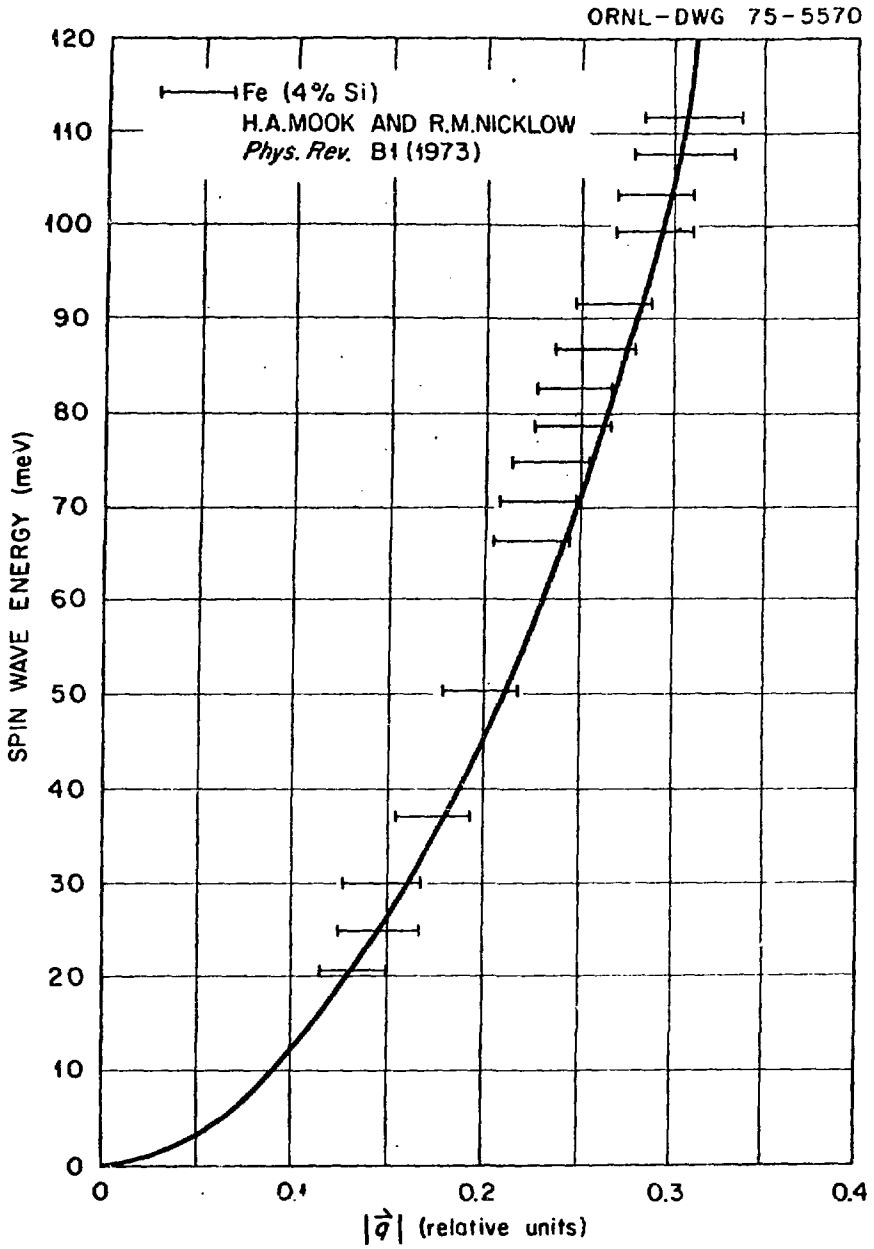
ORNL-DWG 75-5570
Fe (4% Si)
H.A.MOOK AND R.M.NICKLOW
Phys. Rev. B1 (1973)
SPIN WAVE ENERGY (meV)
120
110
100
90
80
70
60
50
40
30
20
10
0
0
0.1
0.2
0.3
0.4
|q| (relative units)

Fig 7